Author(s): Goreshnik, E.A.; Veryasov, G.; Morozov, Dmitry; Slyvka, Yu.; Ardan, B.; Mys'kiv, M.G.

Title: Solvated copper(I) hexafluorosilicate π-complexes based on [Cu2(amtd)2]2+ (amtd = 2-allylamino-5-methyl-1,3,4-thiadiazole) dimer

Year: 2016

Version:

Please cite the original version:

Goreshnik, E.A., Veryasov, G., Morozov, D., Slyvka, Yu., Ardan, B., & Mys'kiv, M.G. (2016). Solvated copper(I) hexafluorosilicate π-complexes based on [Cu2(amtd)2]2+ (amtd = 2-allylamino-5-methyl-1,3,4-thiadiazole) dimer. Journal of Organometallic Chemistry, 810, 1-11. https://doi.org/10.1016/j.jorganchem.2016.03.001

Accepted Manuscript

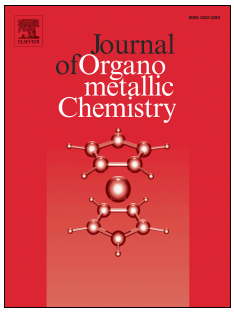

Solvated copper(I) hexafluorosilicate π-complexes based on $[Cu_2(amtd)_2]^{2+}$ (amtd = 2-allylamino-5-methyl-1,3,4-thiadiazole) dimer

Dr. E.A. Goreshnik, G. Veryasov, D. Morozov, Yu. Slyvka, B. Ardan, M.G. Mys'kiv

PII: S0022-328X(16)30075-4

DOI: 10.1016/j.jorganchem.2016.03.001

Reference: JOM 19426

To appear in: *Journal of Organometallic Chemistry*

Received Date: 30 September 2015

Revised Date: 1 March 2016

Accepted Date: 2 March 2016

Please cite this article as: E.A Goreshnik, G Veryasov, D. Morozov, Y. Slyvka, B. Ardan, M.G. Mys'kiv, Solvated copper(I) hexafluorosilicate π-complexes based on $[Cu_2(amtd)_2]^{2+}$ (amtd = 2-allylamino-5-methyl-1,3,4-thiadiazole) dimer, *Journal of Organometallic Chemistry* (2016), doi: 10.1016/j.jorganchem.2016.03.001.

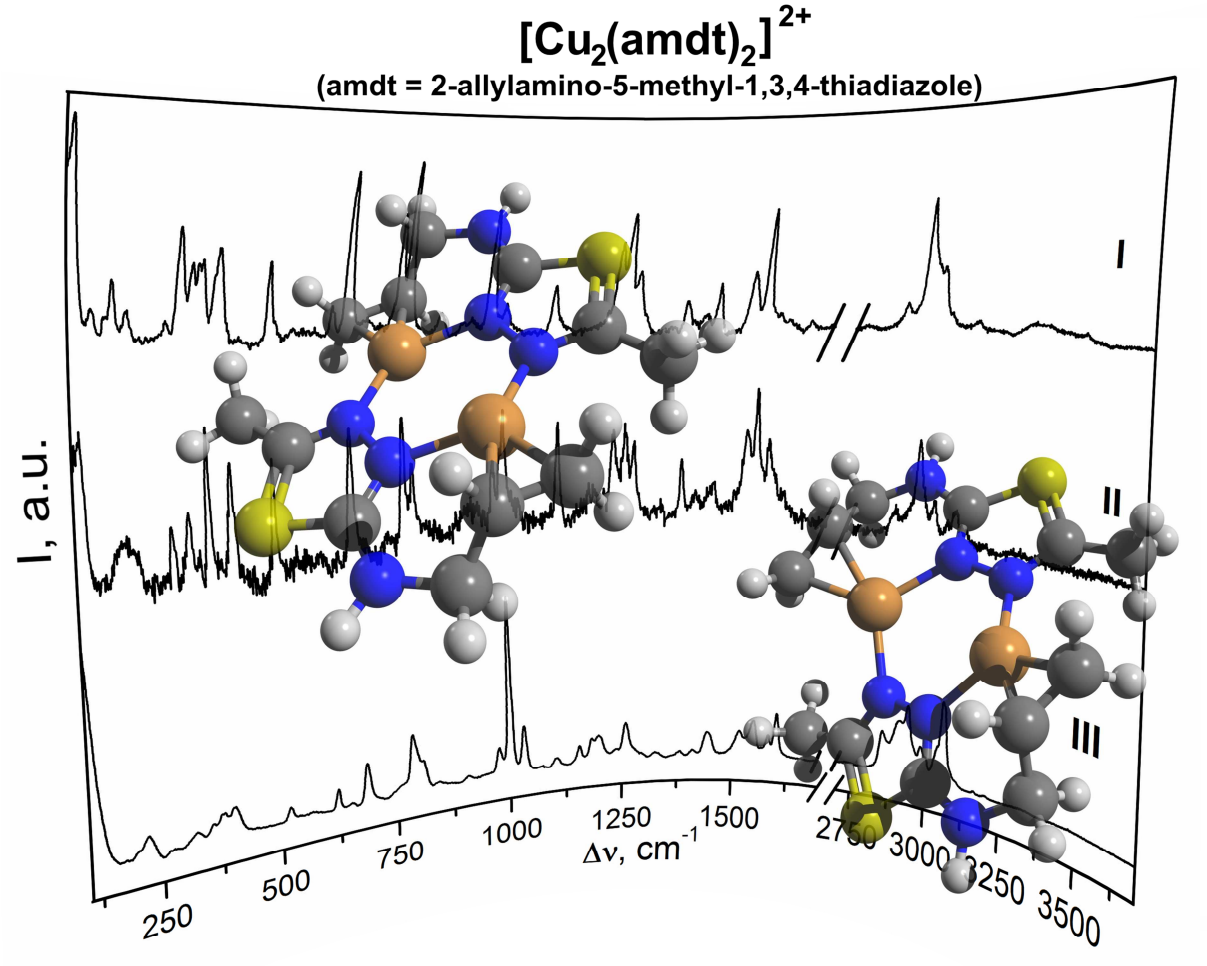

Solvated copper(I) hexafluorosilicate π-complexes based on $[Cu_2(amtd)_2]^{2+}$ (amtd = 2-allylamino-5-methyl-1,3,4-thiadiazole) dimer

E.A. Goreshnik[a*], G.Veryasov[a,b], D. Morozov[c], Yu. Slyvka[d], B. Ardan[d] and M.G. Mys'kiv[d]

[a] Department of Inorganic Chemistry and Technology, Jožef Stefan Institute, Ljubljana, Slovenia

[b] Department of Fundamental Energy Science, Graduate School of Energy Science, Kyoto University, Kyoto, Japan (current affiliation)

[c] Department of Chemistry, Nanoscience center, University of Jyvaskyla, Jyvaskyla, Finland

[d] Department of Inorganic Chemistry, Ivan Franko National University, L'viv, Ukraine

* Dr. E. Goreshnik
Institute Jožef Stefan
Department of Inorganic Chemistry and Technology
Jamova 39, 1000, Ljubljana
Slovenia
Phone: +386 1 477 36 45
Fax: +386 1 477 31 55
Email: evgeny.goreshnik@ijs.si

Abstract.

$[Cu_2(amdt)_2]SiF_6 \cdot C_6H_6$ and $[Cu_2(amdt)_2(H_2O)_2]SiF_6 \cdot CH_3CN \cdot 2H_2O$ (amdt = 2-allylamino-5-methyl-1,3,4-thiadiazole) were obtained by alternating-current electrochemical synthesis, starting from water–acetonitrile–benzene mixtures containing 2-allylamino-5-methyl-1,3,4-thiadiazole and $CuSiF_6 \cdot 4H_2O$. The electrochemical reduction of the saturated copper hexafluorosilicate water solution beneath the neatly poured layer of acetonitrile-benzene amdt solution resulted in the formation of crystalline $[Cu_2(amdt)_2]SiF_6 \cdot C_6H_6$. The initial stirring of the same mixture before subjecting it to the electrochemical reduction resulted in the formation of $[Cu_2(amdt)_2(H_2O)_2]SiF_6 \cdot CH_3CN \cdot 2H_2O$. A sluggish hydrolysis of the acetonitrile over 2 years in a closed test tube with $[Cu_2(amdt)_2]SiF_6 \cdot C_6H_6$ crystals in a mother liquor resulted in the formation of $[Cu_2L_2(H_2O)_2]SiF_6 \cdot CH_3CONH_2 \cdot 2H_2O$. All the compounds were studied using X-ray single-crystal diffraction and Raman spectroscopy. The molecular structures and the Raman spectra of the compounds were discussed on the basis of computational modeling with the DFT/B3LYP/cc-pVDZ method.

Keywords: Copper(I) hexafluorosilicates; Heterocycles; Raman Spectroscopy; Computational modeling.

1. Introduction.

The 1,3,4-thiadiazoles are well known as efficient building blocks for the crystal engineering of metal-organic complexes [1-3]. Soft Lewis acids such as copper(I) have a good affinity for the thiadiazole core and are able to engage in an effective interaction with the C=C bond; therefore, compounds containing both a 1,3,4-thiadiazole ring and a flexible allyl group appear to be suitable for crystal engineering. Despite the fact that allyl derivatives of such a thiadiazole have been known since the 19th Century, crystallographic data on its π-coordination behavior towards transition-metal ions has appeared only recently. Our research has shown the formation of $[Cu_2(amdt)_2]^{2+}$ (amdt = 2-allylamino-5-methyl-1,3,4-thiadiazole) dimers, containing six-membered Cu_2N_4 cycles, completed by various anions [4].

Generally, π-complexes based on the Cu_2SiF_6 salt appear only rarely. Only eight entries corresponding to such compounds were found in the Cambridge Structural Database [5-10]. The fact that just a single compound with the direct Cu^+–SiF_6^{2-} bond is known [9], indicates that the SiF_6^{2-} moiety behaves as a weakly bonded anion with respect to the Cu^+ ion, making the univalent copper cation easily accessible to ligands. The strong affinity of the hexafluorosilicate anion for water frequently leads to the presence of water or other solvent molecules in the crystal structure. For example, in the structure of $[Cu_2(amdt)_2(H_2O)_2]SiF_6\cdot 2.5H_2O$ there are two types of water molecules, i.e., bound to the metal center or attached to the SiF_6^{2-} anions by strong hydrogen bonds [10].

In the present work we report on three new π-coordination compounds containing six-membered Cu_2N_4 cycles formed by two copper(I) ions and two amdt ligands, $[Cu_2(amdt)_2]SiF_6\cdot C_6H_6$, $[Cu_2(amdt)_2(H_2O)_2]SiF_6\cdot CH_3CN\cdot 2H_2O$ and $[Cu_2(amdt)_2(H_2O)_2]SiF_6\cdot CH_3CONH_2\cdot 2H_2O$. The main feature of the benzene-solvated compound $[Cu_2(amdt)_2]SiF_6\cdot C_6H_6$ is the presence of the rarely observed direct Cu^+–SiF_6^{2-} bond. The tetra-hydrated $[Cu_2(amdt)_2(H_2O)_2]SiF_6\cdot CH_3CN\cdot 2H_2O$ and $[Cu_2L_2(H_2O)_2]SiF_6\cdot CH_3CONH_2\cdot 2H_2O$ complexes are solvated by unbound acetonitrile and acetamide molecules, respectively. Presumably, the acetamide appeared as a result of the slow acetonitrile hydrolysis.

2. Results and Discussion

2.1 Crystal structures

Table 1. Crystal data and refinement results for $[Cu_2(amdt)_2]SiF_6 \cdot C_6H_6$ (**I**), $[Cu_2(amdt)_2(H_2O)_2]SiF_6 \cdot CH_3CONH_2 \cdot 2H_2O$ (**II**) and $[Cu_2(amdt)_2(H_2O)_2]SiF_6 \cdot CH_3CN \cdot 2H_2O$ (**III**)

Compound	**I**	**II**	**III**
Formula	$C_{18}H_{24}Cu_2N_6S_2SiF_6$	$C_{14}H_{31}Cu_2F_6N_7O_5S_2Si$	$C_{14}H_{26}Cu_2F_6N_7O_4S_2Si$
FW	657.76	710.77	689.75
Crystal size, mm	0.09 × 0.08 × 0.04	0.58 × 0.19 × 0.14	0.59 × 0.53 × 0.39
Color, shape	Colorless plate	Colorless prism	Colorless block
Temperature, K	200	150	200
Radiation	Mo-K_α	Mo-K_α	Mo-K_α
Sp. gr.	$P\ \bar{1}$	$P2_1/n$	*Fddd*
a, Å	7.8716 (10)	8.0729 (2)	15.9116(5)
b, Å	8.1709 (10)	19.7500 (5)	21.7105 (7),
c, Å	10.3149 (14)	16.3139 (5)	29.1767 (12)
α, deg	111.591 (3)	90.00	90.00
β, deg	110.158 (4)	102.739 (3)	90.00
γ, deg	91.756 (2)°	90.00	90.00
V, $Å^3$	569.59 (13)	2537.08 (12)	10079.1 (6)
Z	1	4	16
D_c g/cm^3	1.917	1.861	1.818
μ, mm^{-1}	2.17	1.97	1.98
Abs. correction	Multi-scan	Analytical	Analytical
Tmin, Tmax	0.829, 0.951	0.530, 0.821	0.429, 0.531
F(000)	332	1448	5584
Diffractometer	Rigaku AFC 7	Agilent Gemini A	Agilent Gemini A
Scan range, θ^o	2.8–28.1	3.7–29.7	3.7–29.4
Reflections	2091	7037	3065
Parameters	161	390	173
R (*F*) [a]	0.053	0.033	0.022
wR^2 [b]	0.148	0.079	0.058
GOF [c]	1.123	1.07	1.05

max. peak &	0.85	0.80	0.81
min. hole, eÅ^{-3}	-0.86	-0.58	-0.35

[a]$R_1 = \Sigma||F_o| - |F_c||/\Sigma|F_o|$ for $I > 2\sigma(I)$. [b]$wR_2 = [\Sigma(w(F_o^2 - F_c^2)^2/ \Sigma(w(F_o^2)^2]^{1/2}$ for $I > 2\sigma(I)$, [c]GOF = $[\Sigma w(F_o^2 - F_c^2)^2) / N_o - N_p)]^{1/2}$, where N_o = no. of reflns and N_p = no. of refined parameters.

The crystal data and refinement results are summarized in Table 1.

2.1.1[Cu_2(amdt)$_2$]SiF_6·C_6H_6

There are at least three unique points that should be highlighted in the structure of the [Cu_2(amdt)$_2$]SiF_6·C_6H_6 compound. The 2-allylamino-5-methyl-1,3,4-thiadiazole plays the role of the N,N,(N-C_3H_5) chelate-bridging ligand connecting two Cu^+ ions into a centrosymmetric dimer Cu_2(amdt)$_2$ (Fig. 1), which contains two six-membered CuC_4N_2 rings (if we consider the C=C bond as a single coordinating site) and one six-membered Cu_2N_4 ring. Similar dimers were previously found in the structure of another N-allylthiadiazole copper(I) complex [Cu_2(amdt)$_2$](CF_3SO_3)$_2$ [10] and in the structure of copper(I) π-complexes with 5-(S-allyl)-1*H*-tetrazole derivatives, where the copper(I) centers connect two of the most nucleophilic N(3) and N(4) atoms in the adjacent tetrazole rings [11, 12]. The copper(I) ion has a trigonal pyramidal environment. Its equatorial plane is arranged by the N atom and the C=C bond from the N-allyl group from one ligand moiety and another N atom from the adjacent thiadiazole core. The next feature of the structure discussed is the presence of a fluorine atom from the SiF_6^{2-} anion at the apical position of the copper coordination sphere. The Cu–F bond length of 2.729(3) Å is noticeably longer than the value of 2.439(2) Å observed earlier in the π-complex of the [Cu_2($C_6H_4N_3$(C_3H_5))$_2$(H_2O)$_2$]SiF_6·2H_2O ($C_6H_4N_3$(C_3H_5) = 1-allylbenzotriazole) composition [9], but still shorter than the sum of the respective VdW radii, i.e., 2.87 Å.

The absence of the direct Cu–F (SiF_6^{2-}) bonds in previously studied Cu_2SiF_6 π-complexes, i.e., [Cu_2(C_3H_5)$_2$NCN(H_2O)$_3$$CH_3OH$][$SiF_6$] [6], [$Cu_2Cl_3$($C_3H_5NH_3$)$_2$]$_2SiF_6$ and [CuOOCH($C_3H_5NH_3$)]$_2SiF_6$ [5], [Cu(H_2O)$_{2.5}$(μ-$C_4H_8N_2$(H)$_2$(C_3H_5)$_2$)$_{0.5}$]SiF_6·H_2O ($C_4H_8N_2$(H)$_2$(C_3H_5)$_2^{2+}$ -diallylpiperazinium) [7], [Cu_2(μ-atu)$_2$(atu)$_4$]SiF_6 (atu = allylthiourea) [13] and [Cu($C_4H_8ONH(C_3H_5)$)(H_2O)$_2$]SiF_6·H_2O ($C_4H_8ONH(C_3H_5)^+$ = N-allylmorpholinium) [8], was attributed to the concept of soft-hard Lewis acids and bases. In general, the soft Lewis

acid Cu^{+} is coordinated by the oxygen atoms from water molecules, whereas the hard base, SiF_6^{2-}, is preferentially bonded with Lewis acids stronger than the Cu^{+}, i.e., hydrogen atoms. $[Cu_2(amdt)_2]SiF_6 \cdot C_6H_6$ appears to be the second reported exception to the general tendency. The first example of a direct Cu^{+}–$F(SiF_6^{2-})$ bond was reported only few years ago [9]. Here we should note that even a single fluoride anion forms a direct bond with the Cu^{+} center, as was observed in the crystal structure of tris(triphenylphosphane) fluorido copper(I) [14, 15]. Probably the reason for the formation of such a bond in $[Cu_2(amdt)_2]SiF_6 \cdot C_6H_6$ is the absence of water in the benzene layer, wherein apparently the reaction occurred. Each SiF_6^{2-} anion acts as a trans-bridge, being bound to two metal centers from different dimers, resulting in the formation of infinite chains. The third, and possibly the most intriguing, peculiarity of this structure is the presence of benzene molecules, included between the above-mentioned chains (Fig. 2; for bond lengths see Table 2). Each benzene ring is located between the two Cu_2N_4 cycles with rather short plane–plane distances of 3.6 Å. The centroid of the benzene ring is located roughly against the N4 atom from the Cu_2N_4 ring (N4…Cg 3.507 Å), and the plane of the benzene ring is very slightly (3.9^{o}) tilted with respect to the metal-organic planes. The value of 3.757(4) Å for the π-π stacking interactions between the benzene and imidazothiadiazole ring systems was reported recently [16]. To the best of our knowledge, there are only two known copper(I) compounds involving the Cu–F (PF_6^{-}) bond and solvated by benzene [17], and only one reported structure of a solvated-by-benzene copper(I) π-complex with a fluorine-containing anion [18].

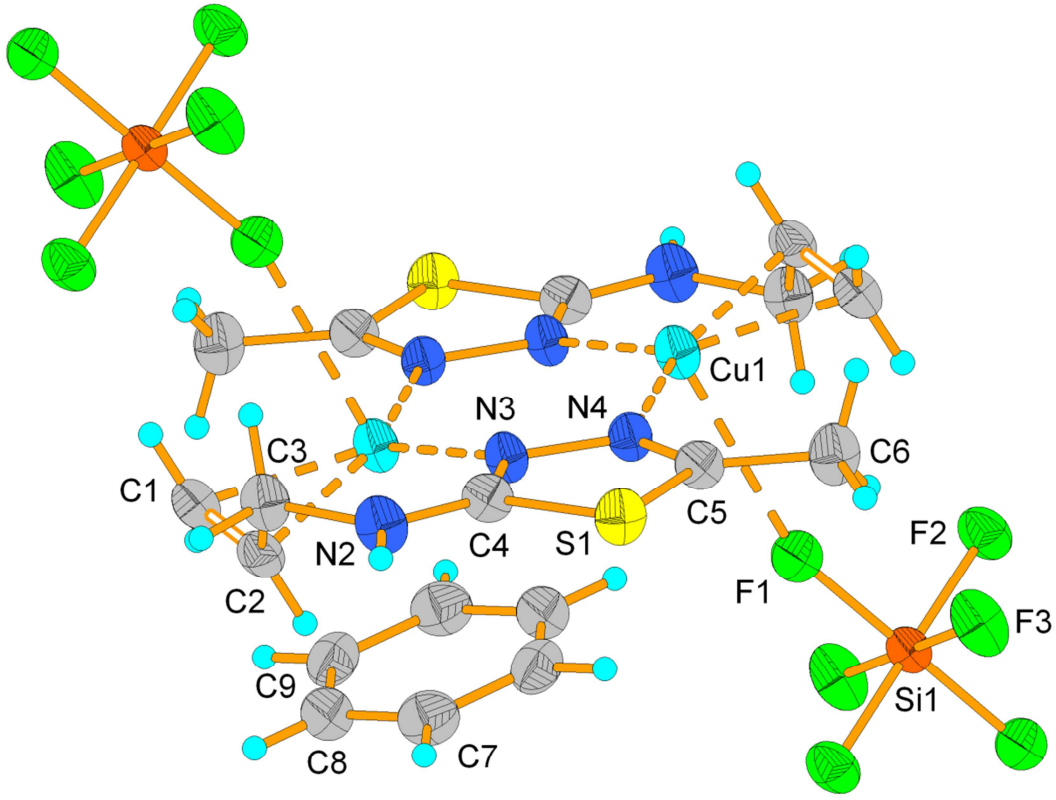

Fig. 1. $[Cu_2(amdt)_2]^{2+}$ dimer with attached SiF_6^{2-} anions and a benzene molecule in the structure of $[Cu_2(amdt)_2]SiF_6 \cdot C_6H_6$ (thermal ellipsoids are drawn for a 50% probability).

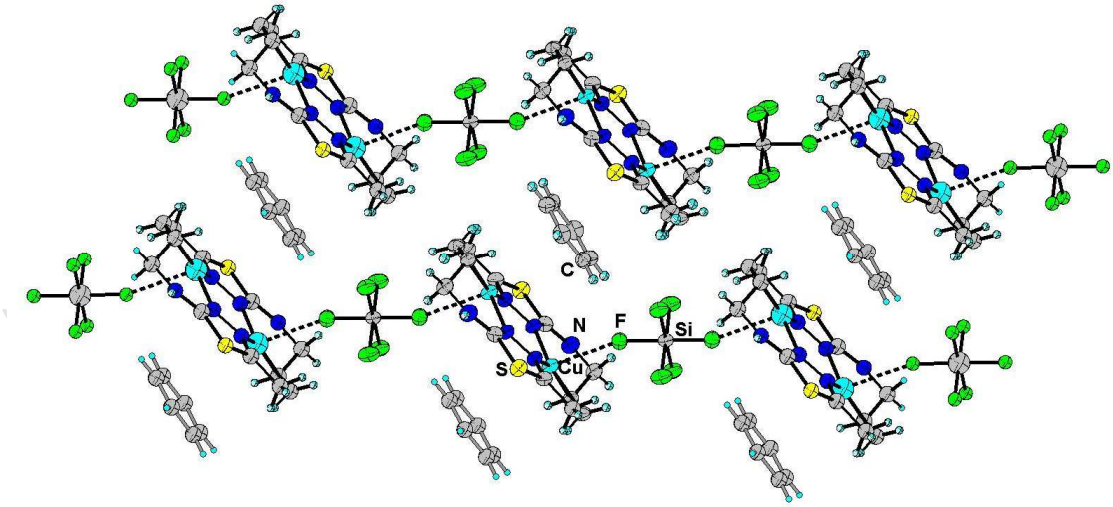

Fig. 2. Benzene molecules between complex chains in the structure of $[Cu_2(amdt)_2]SiF_6 \cdot C_6H_6$.

Table 2. Selected bond distances (Å) in the structure of $[Cu_2(amdt)_2]SiF_6 \cdot C_6H_6$.

Cu1—N4	1.973(3)	N2—C4	1.325(4)
Cu1—N3^{i}	1.987(2)	N2—C3	1.456(4)
Cu1—C2^{i}	2.051(3)	N3—C4	1.324(4)
Cu1—C1^{i}	2.094(3)	N3—N4	1.406(3)
S1—C5	1.732(3)	N4—C5	1.298(4)
S1—C4	1.743(3)	C1—C2	1.363(4)
Si1—F1	1.675(2)	C2—C3	1.522(5)
Si1—F3	1.682(2)	C5—C6	1.494(4)
Si1—F2	1.698(2)	C7—C8	1.382(4)
		C7—C9^{ii}	1.391(5)
		C8—C9	1.374(6)

Symmetry codes: (i) −x+2, −y+1, −z+1; (ii) −x+1, −y+1, −z+1.

From the Dewar–Chatt–Duncanson concept [19] we know that the Cu–(C=C) bond consists of the (Cu^+–L) σ-donor component, formed as a result of the overlapping of the occupied olefin π-orbital and the unoccupied $4s^0$ orbital of the Cu^+ ion, and the Cu^+–(C=C) π-dative component, based on the electron density transferring from the $3d^{10}$ Cu^+ orbitals to the unoccupied antibonding orbital of the C=C group. The σ-component causes a shortening of the Cu–m distance (m is the mid-point of the C=C bond), whereas the π-dative component, being strongly dependent on a proper olefin group orientation in the metal coordination sphere, causes a lengthening of the C=C bond. Therefore, both components affect an increase of the C–Cu–C angle. Thus, a shortening of the Cu–m distance and a lengthening of the C=C distance, together with an increase in the C–Cu–C angle, are useful data for an estimation of the effectiveness of a Cu–(C=C) interaction. An effective Cu–(C=C) interaction leads, in turn, to the transformation of the Cu-atom coordination polyhedron from tetrahedral to trigonal pyramidal, with the olefin group located in the basal plane, and a lengthening of the distance between the metal ion and the axial ligand.

The Cu^+–(C=C) interaction in $[Cu_2(amdt)_2]SiF_6 \cdot C_6H_6$ demonstrates a medium effectiveness. The C–Cu–C angle of 38.4(1)^{o} is usual for such compounds, and the Cu–m distance of

1.957(3) Å appears to be slightly longer than those in earlier explored Cu_2SiF_6 π-complexes (1.920(5) & 1.935(5) Å [9], 1.948(8) Å [10]). The C=C bond coordinated to the copper atom is slightly elongated to 1.363(3) Å, in contrast to the values for free ethylen: 1.338(1) Å (gas phase, [20]), 1.3142(3) Å (at 85 K, [21]) and 1.300 Å in 2-N-allyl-5-phenyl-1,3,4-thiadiazole (RT, [22], it should be noted that the uncoordinated allyl group frequently suffers from partial orientational disordering, resulting in an imaginary shortening of the respective C=C distance). The metal atom resides at the base of the trigonal pyramid and the C=C bond is slightly tilted at 11° relative to the basal plane, as is typical for an effective Cu^+–(C=C) interaction. The observed shift of the C=C stretching band (see below) confirms the medium effectiveness of the Metal–(C=C) interaction.

2.1.2 $[Cu_2(amdt)_2(H_2O)_2]SiF_6{\cdot}CH_3CONH_2{\cdot}2H_2O$

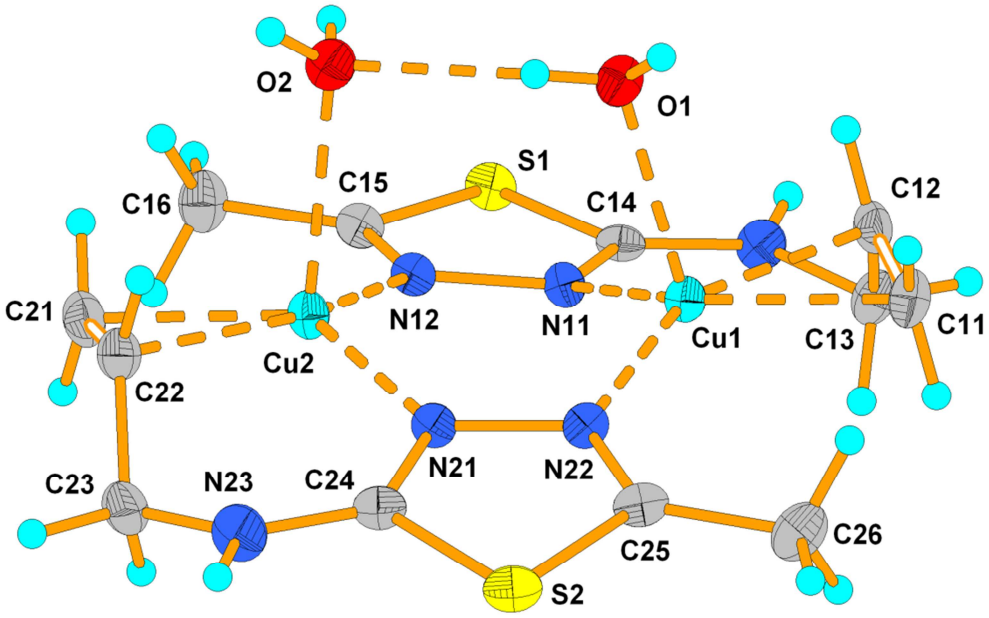

Fig. 3. $[Cu_2(amdt)_2(H_2O)_2]^{2+}$ dimer in the structure $[Cu_2(amdt)_2(H_2O)_2]SiF_6{\cdot}CH_3CONH_2{\cdot}2H_2O$ (thermal ellipsoids are drawn for a 50% probability).

In contrast to $[Cu_2(amdt)_2]SiF_6{\cdot}C_6H_6$, there are two water molecules attached to the Cu^+ centers in the structure of the $[Cu_2(amdt)_2(H_2O)_2]SiF_6{\cdot}CH_3CONH_2{\cdot}2H_2O$ that results in

the acentric $[Cu_2(amdt)_2(H_2O)_2]^{2+}$ cation formation. Both water molecules are located on the same side of the Cu_2N_4 ring. Two other H_2O molecules are not bound to the metal ions and are fixed in the crystal space by hydrogen bonds. Two nitrogen atoms from both thiadiazole cores and a C=C bond form a trigonal surrounding of the copper(I) ion. The oxygen atom from the water molecule completes the trigonal pyramidal metal-coordination sphere. The geometry of the whole dimer is deformed in a "butterfly" mode: both copper ions are shifted from the plane, formed by two pairs of thiadiazole nitrogen atoms, by 0.57 and 0.35 Å, and the planes of the thiadiazole cores are mutually tilted by 18^o (Fig. 3). The absence of an inversion center for the dimer in the $[Cu_2(amdt)_2(H_2O)_2]SiF_6 \cdot CH_3CONH_2 \cdot 2H_2O$ is probably the result of the irregular influence of the doubly-charged SiF_6^{2-} anion on the neighboring Cu^+ ions through hydrogen-bonded H_2O bridge molecules. Very similar dimers were observed previously in the $[Cu_2(amdt)_2(H_2O)_2]SiF_6 \cdot 2.5H_2O$ compound [10]. In both cases two water molecules bound to both metal centers within the dimer are linked by a strong O–H···O hydrogen bond (H···O 1.90 Å, O–H···O 164^o). This H-bond results in a considerable shortening of the O...O distance (2.669(2) Å), in contrast to the Cu...Cu spacing (3.4700(6) Å).

Table 3. Selected bond distances (Å) in the structure of $[Cu_2(amdt)_2(H_2O)_2]SiF_6 \cdot CH_3CONH_2 \cdot 2H_2O$.

Cu1—N22	1.986(2)	S1—C15	1.729(2)
Cu1—N11	2.032(2)	S1—C14	1.737(2)
Cu1—C12	2.057(2)	S2—C25	1.725(2)
Cu1—C11	2.077(2)	S2—C24	1.737(2)
Cu1—O1	2.234(2)	N11—N12	1.399(2)
Cu2—N12	1.993(2)	N12—C15	1.298(3)
Cu2—N21	2.015(2)	N13—C14	1.329(3)
Cu2—C22	2.058(2)	N13—C13	1.461(3)
Cu2—C21	2.080(2)	N21—C24	1.327(3)
Cu2—O2	2.394(2)	N21—N22	1.402(2)
Si1—F3	1.658(1)	N22—C25	1.298(3)
Si1—F2	1.679(2)	N23—C24	1.330(3)
Si1—F5	1.689(1)	N23—C23	1.459(3)
Si1—F4	1.693(1)	C1—C2	1.498(3)
Si1—F1	1.694(1)	C11—C12	1.360(3)

Si1—F6	1.718(1)	C12—C13	1.501(3)
O5—C1	1.245(3)	C15—C16	1.491(3)
N1—C1	1.330(3)	C21—C22	1.360(3)
N11—C14	1.322(2)	C22—C23	1.499(3)

The main difference between $[Cu_2(amdt)_2(H_2O)_2]SiF_6 \cdot CH_3CONH_2 \cdot 2H_2O$ and the previously studied "water" complex [10] is the presence of the acetamide molecule attached via the O–H···O and N–H···O hydrogen bonds to the pair of H_2O molecules (Fig. 4). It appears that the mentioned Ow...Ow distance is the most suitable for an effective bonding to the O=C–NH_2 fragment with a N...O distance of 2.257(3) Å. Such a similarity, like in a key-lock pair, results in the effective implementation of the acetamide molecule into the crystal structure. The appearance of acetamide molecules as a product of acetonitrile hydrolysis was previously observed, for example, during the synthesis of $[C_2H_6ON]_2[Cu_2Cl_2(\mu\text{-}CH_3COO)_4]$ [23]. The Cu^+ ions in $[Cu_2(amdt)_2(H_2O)_2]SiF_6 \cdot CH_3CONH_2 \cdot 2H_2O$ are shifted from the basal plane of the coordination polyhedron by 0.25 and 0.28 Å, and the Cu–O distances are noticeably different (2.234(2) Å and 2.394(2) Å, Table 3). Elongated to 1.360(3) Å, the coordinated C=C bonds are slightly tilted (C11=C12 by 7.6°, C21=C22 9.8°) relative to the basal plane of the coordination polyhedron. The SiF_6^{2-} anion forms two O–H···F (with one metal-anchored and one "free" water molecule) and three N–H···F (two from the amino group, from two different dimers, and one from the acetamide moiety) hydrogen bonds. The shortest Si–F bond length corresponds to the fluorine atom, which does not form a hydrogen bond. Owing to such SiF_6^{2-} bridge dimers, the water molecules and acetamide units are interconnected into a three-dimensional network.

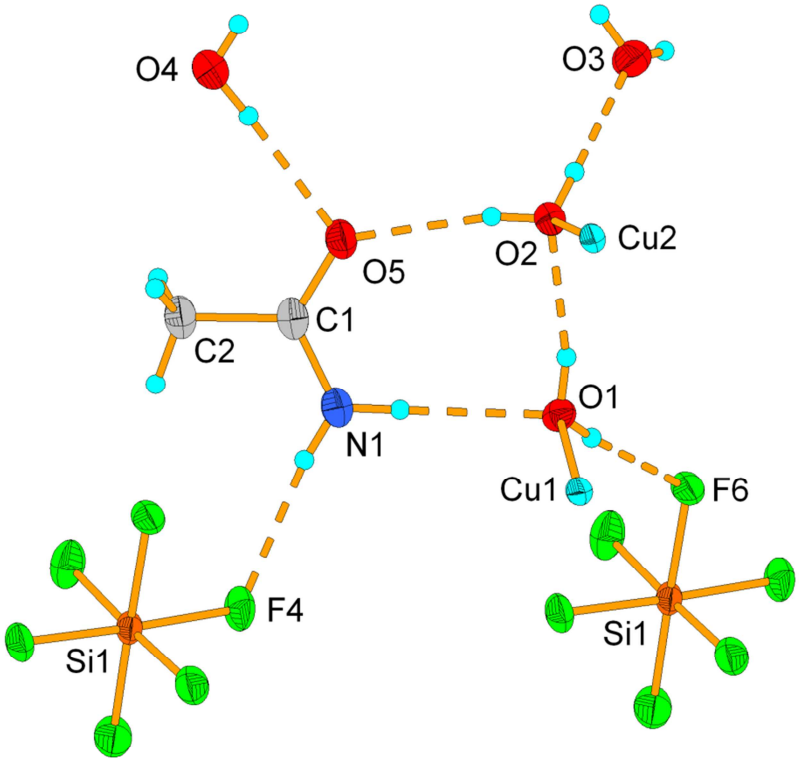

Fig. 4. System of hydrogen bonds in the structure $[Cu_2(amdt)_2(H_2O)_2]SiF_6 \cdot CH_3CONH_2 \cdot 2H_2O$ (thermal ellipsoids are drawn for a 50% probability).

2.1.3 $[Cu_2(amdt)_2(H_2O)_2]SiF_6 \cdot CH_3CN \cdot 2H_2O$

Similar to $[Cu_2(amdt)_2(H_2O)_2]SiF_6 \cdot CH_3CONH_2 \cdot 2H_2O$, acentric dimers were also observed in the structure of the compound $[Cu_2(amdt)_2(H_2O)_2]SiF_6 \cdot CH_3CN \cdot 2H_2O$. These cationic units are markedly distorted: the planes of two thiazole cores are noticeably twisted (torsion angle N1–N2–N1'–N2' is 18.1°), and both metal ions are shifted from the plane of the dimer (Fig. 5; for the bond lengths, see Table 4). The Cu–N and Cu–O distances are very similar to those in $[Cu_2(amdt)_2(H_2O)_2]SiF_6 \cdot CH_3CONH_2 \cdot 2H_2O$. Coordinated to the copper center, the C=C bond has a length of 1.367(3) Å.

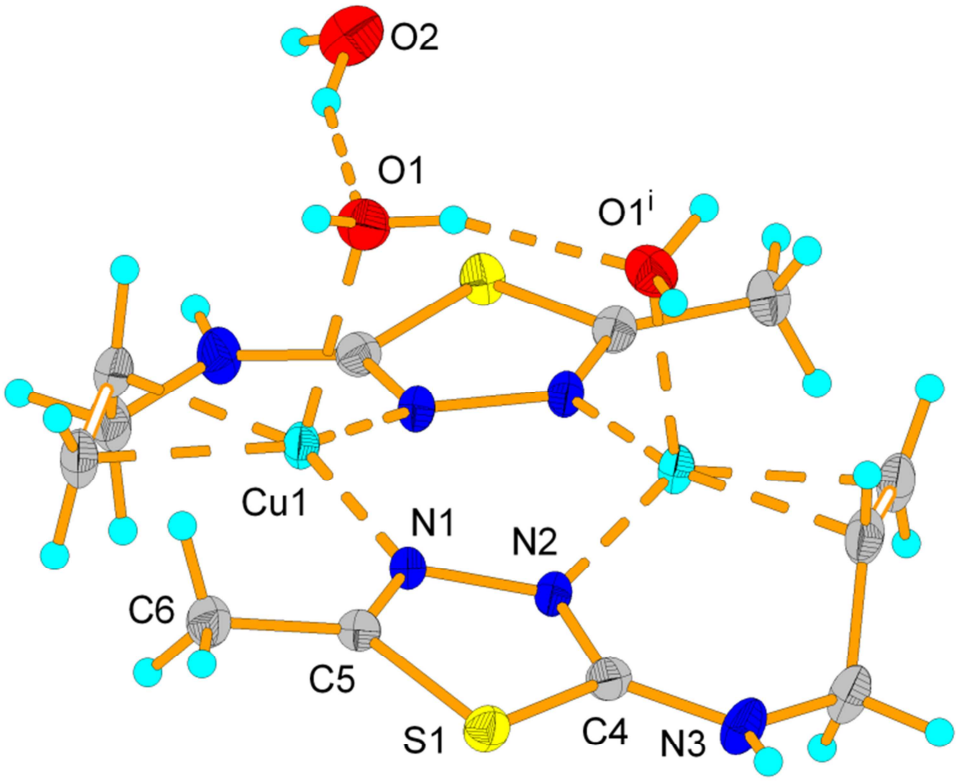

Fig. 5. $[Cu_2(amdt)_2(H_2O)_2]^{2+}$ dimer and "free" water molecule (O2) in the structure of $[Cu_2(amdt)_2(H_2O)_2]SiF_6 \cdot CH_3CN \cdot 2H_2O$ (thermal ellipsoids are drawn for a 50% probability). Only one water-molecule orientation is shown (see text below).

Table 4. Selected bond distances (Å) in the structure of $[Cu_2(amdt)_2(H_2O)_2]SiF_6 \cdot CH_3CN \cdot 2H_2O$.

Cu1—N1	1.979(2)	N1—C5	1.293(2)
Cu1—N2^{i}	2.021(2)	N1—N2	1.406(2)
Cu1—C2^{i}	2.046(2)	N2—C4	1.320(2)
Cu1—C1^{i}	2.087(2)	N3—C4	1.330(2)
Cu1—O1	2.327(2)	N3—C3	1.459(2)
S1—C5	1.726(2)	N4—C8	1.138(7)
S1—C4	1.734(2)	C1—C2	1.367(3)
Si1—F2	1.674(1)	C2—C3	1.491(3)
Si1—F3	1.675(1)	C5—C6	1.496(3)
Si1—F1	1.690(1)	C7—C8	1.513(6)

Symmetry codes: (i) x, −y+3/4, −z+3/4; (ii) −x+3/4, y, −z+3/4; (iii) −x+3/4, −y+3/4, z.

The two crystallographically independent water molecules in $[Cu_2(amdt)_2(H_2O)_2]SiF_6 \cdot CH_3CN \cdot 2H_2O$ differ greatly in terms of their bonding modes. One of them is attached to the copper atom, whereas the other one is fixed in the crystal structure via the O–H···F and O–H···O hydrogen bonds (Fig. 6). The SiF_6^{2-} anion forms, besides O–H···F, a pair of weak N–H···F bonds. The most interesting peculiarity of the discussed structure is the presence of an uncoordinated acetonitrile molecule, disordered in an unusual manner: two half-occupied nitrile groups are nearly perpendicularly oriented and bound to the common methyl group (Fig. 7). The acetonitrile molecules are located between two dimers, close to the "empty" side of each dimer. The appearance of the non-bonded acetonitrile in the crystal structure of the copper(I) complexes containing a fluorinated anion was described earlier [24].

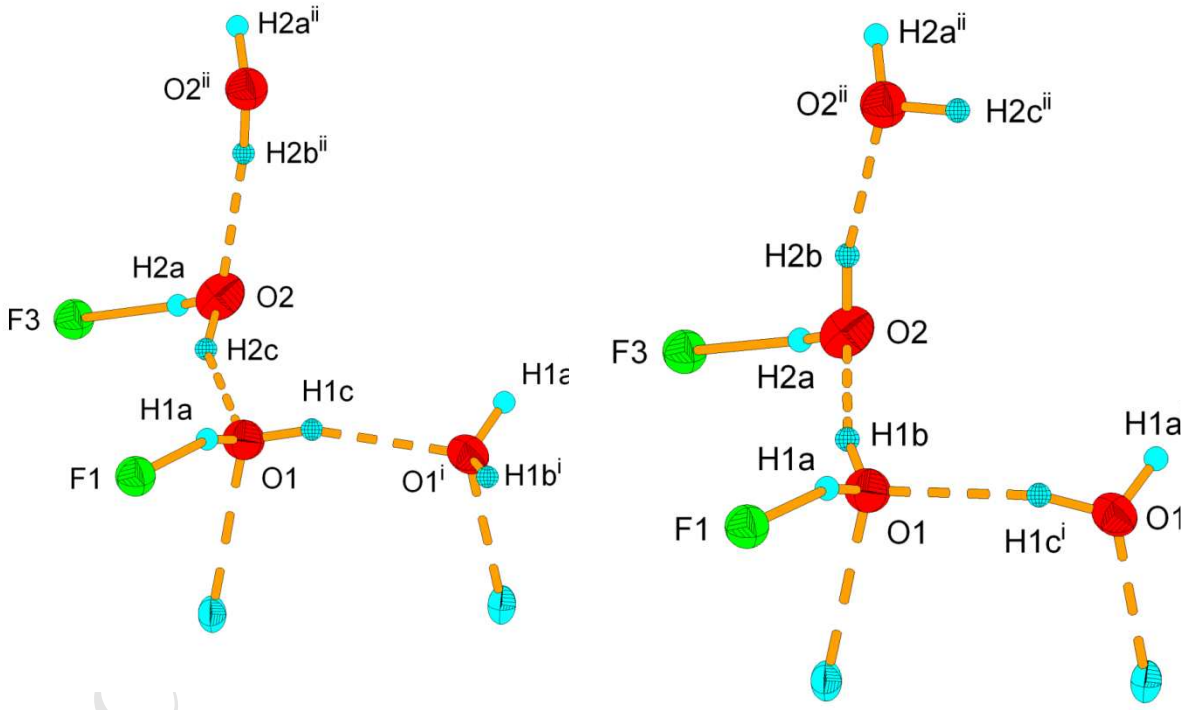

Fig. 6. Two "resonance" structures containing disordered water molecules. The hydrogen atoms with full occupancy are shown as empty balls; the H-atoms with occupancy ½ are drawn as hatched circles.

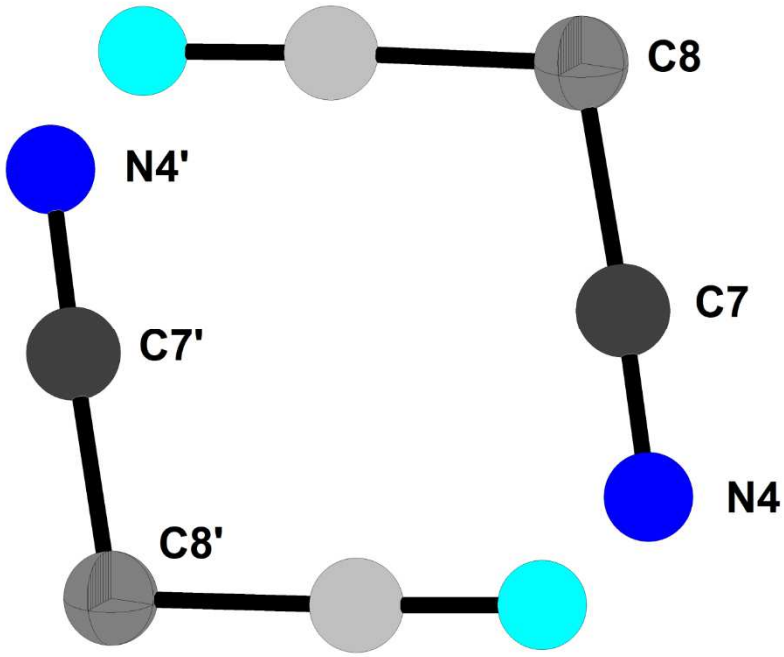

Fig. 7. Disordered acetonitrile molecules in $[Cu_2(amdt)_2(H_2O)_2]SiF_6 \cdot CH_3CN \cdot 2H_2O$. One orientation of the C7 and N4 atoms and their symmetrically generated analogues are indicated by darker colors, another disordered part is indicated by lighter colors, and its atoms are drawn without labels.

A correct determination of the positions of the water's hydrogen atoms was problematic. For each of the O1 and O2 atoms only one neighboring hydrogen atom that participated in the formation of the O–H···F hydrogen bond was found on the difference Fourier map. All attempts to locate the position of the other two hydrogens resulted in too short H…H distances between the symmetrically generated atoms. The worst results appear with the location of the desired hydrogen atoms near the imaginary line connecting pairs of symmetrically generated O1–O1' and O2–O2' atoms. On the other hand, considerable shortening of the O1–O1' distance, in comparison to the corresponding Cu–Cu1' distance, clearly indicates the existence of an O1–H···O1' hydrogen bond, similar to that in the structure of the compound $[Cu_2(amdt)_2(H_2O)_2]SiF_6 \cdot CH_3CONH_2 \cdot 2H_2O$. To resolve this contradiction, a model with disordered water molecules was built. In such a model each oxygen atom has three H neighbors: one of them (i.e., H1a and H2a), directed to the closest fluorine atom, has an occupancy of 1, all the others have an occupancy of ½. The two

"resonance" structures derived from the model are shown in Fig. 7. Such a model satisfactorily explains the O...O distances that are usual for water molecules connected via O–H···O hydrogen bonds. Details about the hydrogen bonds observed in the discussed compounds are summarized in Table 5.

Table 5. Hydrogen-bond geometries in the compounds $[Cu_2(amdt)_2]SiF_6 \cdot C_6H_6$, $[Cu_2(amdt)_2(H_2O)_2]SiF_6 \cdot CH_3CONH_2 \cdot 2H_2O$ and $[Cu_2(amdt)_2(H_2O)_2]SiF_6 \cdot CH_3CN \cdot 2H_2O$.

$[Cu_2(amdt)_2]SiF_6 \cdot C_6H_6$				
D—H···*A*	*D*—H	H···*A*	*D*···*A*	∠*D*—H···*A*
N2—H1N2···F2	0.86	2.11	2.855(3)	144.7
N2—H1N2···F3	0.86	2.11	2.865(3)	145.5
$[Cu_2(amdt)_2(H_2O)_2]SiF_6 \cdot CH_3CONH_2 \cdot 2H_2O$				
O1—H1*B*···O2	0.79(3)	1.91(3)	2.671(2)	164(3)
O1—H1A···F6	0.76(3)	1.93(3)	2.684(2)	173(3)
O2—H2A···O3^{i}	0.81(3)	1.89(3)	2.702(2)	178(3)
O2—H2B···O5^{ii}	0.78(4)	2.06(4)	2.824(2)	169(3)
O3—H3B···F1	0.73(3)	2.08(4)	2.804(2)	172(4)
O3—H3A···O4	0.83(4)	1.97(4)	2.797(3)	175(3)
O4—H4A···O5	0.81(4)	2.08(4)	2.890(3)	177(4)
N13—H13···F5^{iii}	0.77(3)	2.18(3)	2.860(2)	148(3)
N23—H23···F2^{iv}	0.79(3)	2.10(3)	2.853(2)	159(3)
N1—H1D···O1^{v}	0.84 (3)	2.13 (3)	2.970 (3)	178(3)

Symmetry codes: (i) −*x*+3/2, *y*+1/2, −*z*+1/2; (ii) −*x*+1/2, *y*+1/2, −*z*+1/2; (iii) *x*−1, *y*, *z*; (iv) *x*+1/2, −*y*+3/2, *z*+1/2; (v) −*x*+1/2, *y*−1/2, −*z*+1/2.

$[Cu_2(amdt)_2(H_2O)_2]SiF_6 \cdot CH_3CN \cdot 2H_2O$				
O1—H1*B*···O2^{i}	0.79(3)	2.14(6)	2.810(3)	143(9)
O1—H1*A*···F1^{iv}	0.74(2)	2.09(2)	2.809(2)	163(3)
O2—H2*B*···F3^{v}	0.76(2)	2.36(2)	3.105(3)	166(4)
N3—H3···F2^{v}	0.86	2.23	3.021(2)	152
N3—H3···F1^{v}	0.86	2.22	2.943(2)	142

Symmetry codes: (i) *x*, −*y*+3/4, −*z*+3/4; (iv) −*x*+5/4, −*y*+5/4, *z*; (v) −*x*+1, −*y*+1, −*z*+1.

2.2 Geometry optimization

Computational modeling was performed on the $[Cu_2(amdt)_2]^{2+}$ cation, since it is the element that is present in all the structures and the residual fragments, i.e., the SiF_6^{2-} anions and the coordinated solvent molecules, are of little interest. The geometry optimization with DFT/B3LYP/cc-pVDZ converged to the energy minimum; the structure of the cation at the

stationary point in comparison to the experimental geometries is shown at Fig. 8 (a new atom-numbering scheme was applied for convenience).

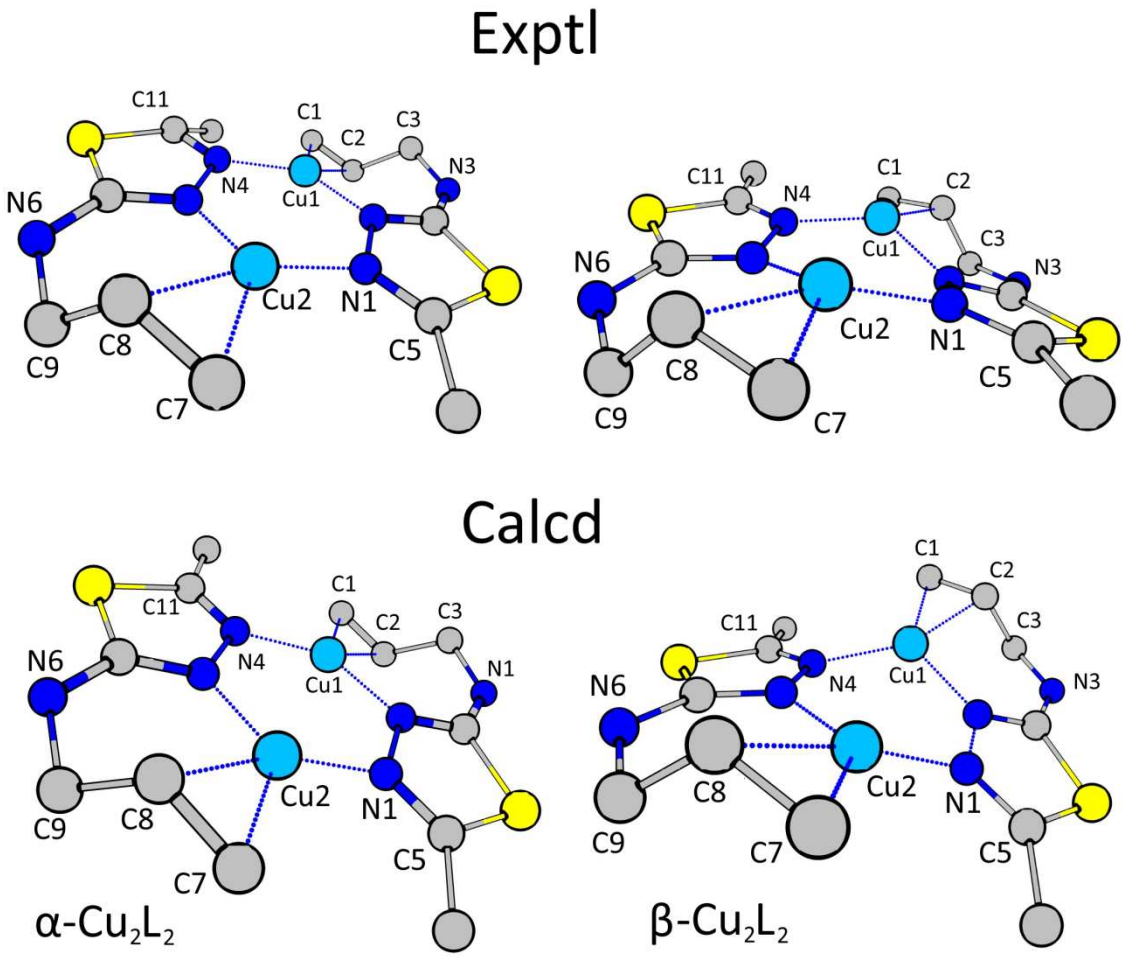

Fig. 8. Schematic ball-and-stick models of the experimental and computed geometries of **α**-(left, observed in $[Cu_2(amdt)_2]SiF_6 \cdot C_6H_6$) and **β**-(right, observed in compounds $[Cu_2(amdt)_2(H_2O)_2]SiF_6 \cdot CH_3CONH_2 \cdot 2H_2O$ and $[Cu_2(amdt)_2(H_2O)_2]SiF_6 \cdot CH_3CN \cdot 2H_2O$); the experimental geometry of the dimeric cation in $[Cu_2(amdt)_2(H_2O)_2]SiF_6 \cdot CH_3CONH_2 \cdot 2H_2O$ is represented in the figure $[Cu_2(amdt)_2]^{2+}$, the hydrogen atoms and double bonds are omitted for clarity.

Table 6. Comparison of selected bonds (Å) and angles (°) in the experimental (exptl) and equilibrium (calcd) geometries of the **α** (compound $[Cu_2(amdt)_2]SiF_6 \cdot C_6H_6$ (**I**)) and **β** (compounds $[Cu_2(amdt)_2(H_2O)_2]SiF_6 \cdot CH_3CONH_2 \cdot 2H_2O$ (**II**) and $[Cu_2(amdt)_2(H_2O)_2]SiF_6 \cdot CH_3CN \cdot 2H_2O$ (**III**)).

bond, angle	**α**-$[Cu_2(amdt)_2]$		**β**-$[Cu_2(amdt)_2]$		
	calcd	exptl (**I**)	calcd	exptl (**II**)	exptl (**III**)
C1-C2, C7-C8	1.374	1.363(4)	1.379	1.360(3)	1.367(3)
C2-C3, C7-C8	1.510	1.522(5)	1.510	1.501(3)	1.490(3)
C3-N3, C9-N6	1.466 1.465	1.456(4)	1.471	1.461(3)	1.459(3)
C2-C3-N3, C8-C9-N6	112.3 112.1	111.9(3)	113.2	114.2(2)	113.2(2)
Cu1-N4-C11, Cu2-N1-C5	127.6 127.4	127.2(2)	129.2	129.4(1)	128.1(1)
Cu2-N1, Cu1-N4	1.999 2.039	1.973(3)	2.005	1.984(3)	1.979(2)

The equilibrium geometries obtained through the optimization appear to be close to the experimental ones. The XYZ files containing the computed and initial geometries are available in the supporting info. The angles C8–C9–N6 and C2–C3–N3 for **α**-$[Cu_2(amdt)_2]^{2+}$ have values of 111.8(2)° in the experiment and 112.26° and 112.12° in the computation. The main difference between the two cations, which demanded a separate examination of the cations, is the relative positioning of the C8–C9–N6 and C2–C3–N3 fragments (see Figure 8). If considered from the point of view of the relative arrangement of the substituents on the two C=C groups (C1–C2 and C7–C8), bonded to the copper atoms, these isomers could be crudely called *trans* (for **α**-$Cu_2(amdt)_2$) and *cis* (for **β**-$Cu_2(amdt)_2$), since C3 and C9 are located at the *trans*- positions in the **α**-$Cu_2(amdt)_2$ and at the *cis* positions in the **β**-$Cu_2(amdt)_2$. It should be noted that the geometry optimization resulted in a tilt of the ligand

molecules in the **β**-$Cu_2(amdt)_2$ caused by the Coulomb interactions of the methyl and allyl groups. The torsion angle between the planes formed by C7, Cu2, N1 and Cu2, N1, C5 (or another set C1, Cu1, N4 and Cu1, N4, C11) changed from -14.1° to 19.5° (Δ = 33.6°), giving the cation a saddle-shaped conformation. For **α**-Cu_2L_2 no such changes were observed.

2.3 Raman spectroscopy

The Raman spectra, calculated from the optimized geometry, had no imaginary frequencies, indicating that the equilibrium geometry was determined correctly. Simulated spectra were used for the detailed vibrational band assignments of the experimental spectra.

In our previous experience with Cu^+ coordination compounds [25] it was established that a Raman spectra could be measured directly in the air without decomposition; however, the laser power has to be reduced to 1.7 mW using a density filter. The recorded Raman spectra for all of the compounds are shown at Fig. 9; the part 1750–2700 cm^{-1} is omitted for convenience. Among all the spectra, only the C–N stretching band from the acetonitrile, which is present in the compound $[Cu_2(amdt)_2(H_2O)_2]SiF_6 \cdot CH_3CN \cdot 2H_2O$, emerged at 2245 cm^{-1} (see Fig. S1, Supplementary materials). The spectra are relatively complicated due to the number of bands appearing from the organic ligand. For a clearer representation, the bands with relative intensities and assignments that are based on a simulated spectrum are listed in Tables 6 and 7. The computed bands are omitted in Table 7 due to the low level of interest and the discrepancies in the C–H, O–H and N–H stretching band positions and intensities.

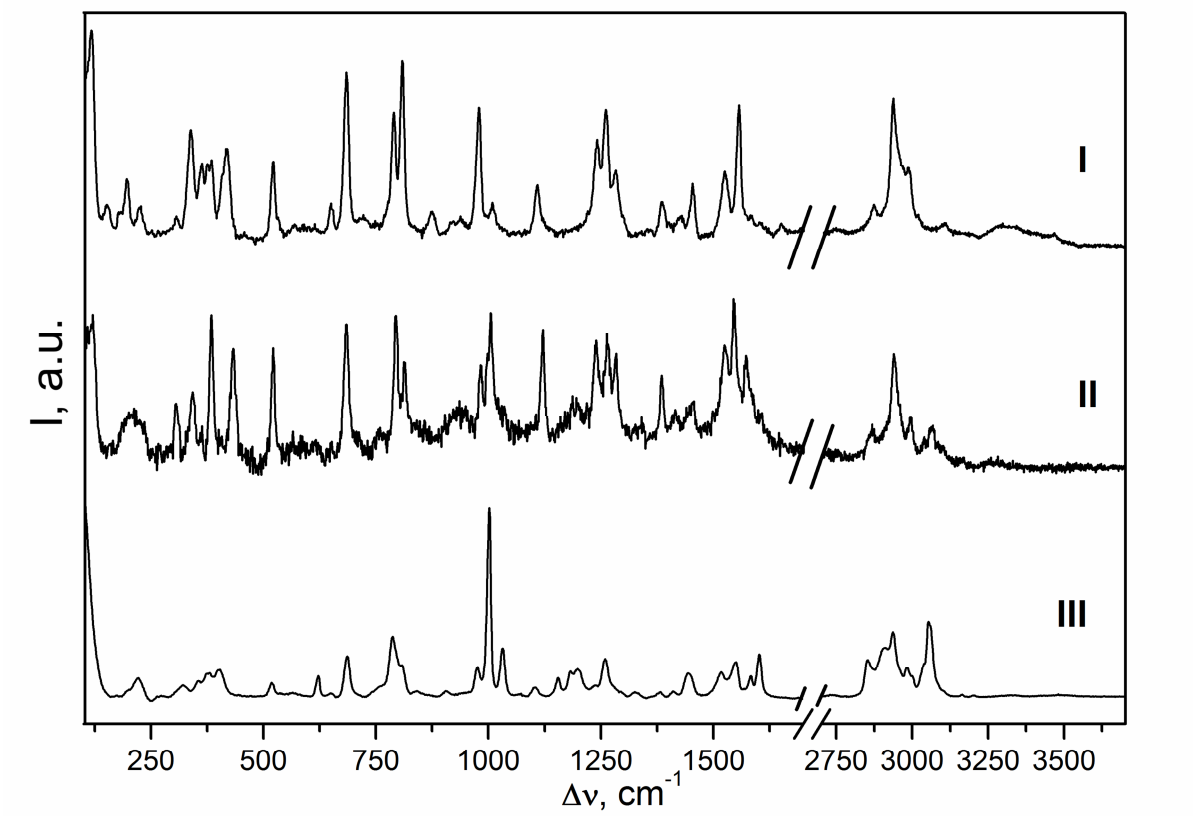

Fig. 9. Raman spectra of the compounds $[Cu_2(amdt)_2]SiF_6 \cdot C_6H_6$ (**I**), $[Cu_2(amdt)_2(H_2O)_2]SiF_6 \cdot CH_3CONH_2 \cdot 2H_2O$ (**II**) and $[Cu_2(amdt)_2(H_2O)_2]SiF_6 \cdot CH_3CN \cdot 2H_2O$ (**III**)

For a description of the bands that appear from the solvents, i.e., benzene, which is present in the structure of the compound $[Cu_2(amdt)_2]SiF_6 \cdot C_6H_6$ [26], acetamide, in the structure of the compound **II** [27], and acetonitrile, for compound **III** [26], we referred to the literature data. For the assignments of the bands resulting from the SiF_6^{2-} anion, we referred to the article by A. Ouasri et al. [28].

The geometry of the **α**-cation (the **α** and **β** designations are added for convenience in the discussion) is characteristic for **I**, and **β** is characteristic for **II** and **III**. The spectra are

relatively complicated, so precise descriptions of each vibrational band were omitted for clarity.

The most intense bands appeared at 115 cm^{-1} and 100 cm^{-1} in the case of compounds **II** and **III**, and are due to the breath deformations of the cation; for the compound **I** the same band appeared at 117 cm^{-1} with a relative intensity 0.90 and the most intense one was observed at 1541 cm^{-1} and refers to the C–N stretching frequency. It should be noted that there is clear tendency for a lowering of the intensity for the ν(C-N) bands in the sequence **I** > **II** > **III,** which is presumably caused by the influence of the screening effect of the anions and the stronger 3D network formed by the hydrogen bonds.

The C=C stretching bands, which are frequently used for the characterization of compounds with allyl groups, appeared at 1620 cm^{-1}, 1647 cm^{-1} and 1603 cm^{-1} for the compounds **I**, **II** and **III** respectively. Presumably, the different shifts towards lower frequencies are caused by the different connectivities of the SiF_6^{2-} anions. The corresponding band in a free ligand was observed at 1637 cm^{-1}.

Table 7. Raman spectra of $[Cu_2(amdt)_2]SiF_6 \cdot C_6H_6$ (**I**), $[Cu_2(amdt)_2(H_2O)_2]SiF_6 \cdot CH_3CONH_2 \cdot 2H_2O$ (**II**) and $[Cu_2(amdt)_2(H_2O)_2]SiF_6 \cdot CH_3CN \cdot 2H_2O$ (**III**) and the computed Raman spectrum of $[Cu_2(amdt)_2]^{2+}$ with band assignments in the range 100–1700 cm^{-1}

I		calcd **α**		**II**		**III**		calcd **β**		Assignments
pos[a]	int[b]	pos[a]	int[b]	pos[a]	int[b]	pos[a]	int[b]	pos[a]	int[b]	
117	0.90	132	1.00	113	1.00	100	1.00	96	0.32	δ_b
				148	0.15			138	0.15	τ
				176	0.11			174	0.16	δ_b
				192	0.28			193	0.12	δ_{lig}
213	0.27	233	0.12	221	0.13	222	0.10	204	0.14	δ_{lig}
302	0.31	311	0.35	302	0.10	321	0.07	286	0.38	ν(Cu-C)
339	0.37	344	0.54	335	0.52			325	0.56	ν(Cu-C)
				359	0.36	355	0.09	329	0.06	ν(Cu-C)
				372	0.35			374	0.49	ν(Cu-C)
381	0.88	380	0.28	380	0.37	377	0.12	379	0.04	ν(Cu-C)+δ(N-C-C)‡
429	0.67	420	0.03	413	0.42	401	0.14	393	0.90	ν(Cu-C)
518	0.68	517	0.20	518	0.36	518	0.08	513	0.49	δ(C-S-C)
						566	0.03	579	0.05	δ(N-C-C)
				646	0.16					ν(C-S)
680	0.83	690	0.18	681	0.78	686	0.21	682	0.71	ν(C-S)+ν(Si-F)
		691	0.29							
790	0.89	792	0.21	718	0.10			707	0.17	ν(S-CH_3)+ν(Si-F)
		796	0.24	786	0.60	787	0.31	795	0.73	w(C-H)$_{al}$
809	0.58	812	0.05	805	0.85	808	0.17	812	0.24	ν(Cu-N)+δ(C-H)†*
		814	0.17	871	0.12	842	0.04	898	0.03	
931	0.25	904	0.01	934	0.10	905	0.04	956	0.10	w(C-H)$_{al}$
		906	0.01							
979	0.56	973	0.15	975	0.62	976	0.16	974	0.29	w(C-H)$_{al}$
		987	0.13							

1001	0.91	1007	0.05	1005	0.15	1002	0.96	1009	0.14	w(C-H)+w(C-H)*+ν(ring)†
		1013	0.02			1032	0.25	1030	0.02	w(C-H)
1117	0.76	1133	0.22	1105	0.25	1105	0.45	1105	0.06	ν(N-N)
						1155	0.10	1143	0.25	ν(C-C)
								1144	0.03	
						1192	0.13			ν(C-C)
						1199	0.15			ν(C-C)
1184	0.28									δ(C-H)†
		1224	0.08							ν(C-C)
1236	0.72	1233	0.03							ν(C-C)
		1235	0.01	1238	0.47	1237	0.06	1226	0.07	ν(C-N)
1259	0.77	1256	0.37	1257	0.61	1260	0.20	1261	0.34	ν(C-C) allyl
		1258	0.16							
		1260	0.15							
1280	0.64	1276	0.19	1279	0.32			1276	0.62	$\nu(C\text{-}C)_{al}$ + δ(C-H)†
		1283	0.17							
						1325	0.03	1344	0.04	w(C-H) + w(N-H)
1381	0.50	1390	0.06	1380	0.15	1383	0.03	1395	0.39	w(C-H) + w(N-H)
1411	0.27	1425	0.07	1423	0.10	1411	0.04	1424	0.17	w(C-H)
		1429	0.06							
1450	0.32	1453	0.04	1450	0.24	1443	0.13	1444	0.22	w(C-H) + w(C-H)*
		1457	0.05							
1521	0.69	1521	<0.01	1522	0.31	1518	0.76	1521	0.04	w(N-H)
1541	1.00	1554	0.30	1553	0.64	1583	0.11	1586	0.62	ν(C-N)
		1555	0.06							
1569	0.63	1617	0.01	1579	0.10			1617	0.01	ν(C-N) + ν(ring)†
		1620	0.20	1647	0.06	1603	0.22	1620	0.50	$\nu(C\text{-}N)+\delta(H_2O)+\nu(C{=}C)_{al}$

[a] – band positions are given in cm^{-1}, [b] – relative intensities (maximum -1.00), ip – in-plane, oop – out-of-plane, ν – stretch, w – wagging, τ – torsion, δ – bending, r – rocking, δ_b -breath, $_{al}$ - allyl

† denotes bands from benzene (**I**), * denotes bands from acetamide (**II)** ‡ denotes bands from acetonitrile (**III)**

Table 8. Experimental Raman spectra of $[Cu_2(amdt)_2]SiF_6 \cdot C_6H_6$ (**I**), $[Cu_2(amdt)_2(H_2O)_2]SiF_6 \cdot CH_3CONH_2 \cdot 2H_2O$ (**II**) and $[Cu_2(amdt)_2(H_2O)_2]SiF_6 \cdot CH_3CN \cdot 2H_2O$ (**III**) in the range 2650–3500 cm^{-1}

I		**II**		**III**		Assignments
pos	int	pos	int	pos	int	
2682	0.17			2852	0.20	
		2868	0.15	2908	0.26	
2934	0.62	2932	0.67	2937	0.34	
2990	0.21	2979	0.33	2981	0.16	
3061	0.16	3012	0.10	2999	0.11	ν(C-H)
		3281	0.05	3039	0.17	
				3054	0.39	
				3164	0.01	
				3202	0.01	
3463	0.06	3451	0.01	3481	0.01	ν(N-H)

ν – stretching

3. Conclusions

We report on synthesis and characterization of three novel copper(I) coordination compounds, i.e., $[Cu_2(amdt)_2]SiF_6 \cdot C_6H_6$, $[Cu_2(amdt)_2(H_2O)_2]SiF_6 \cdot CH_3CONH_2 \cdot 2H_2O$ and $[Cu_2(amdt)_2(H_2O)_2]SiF_6 \cdot CH_3CN \cdot 2H_2O$ (amdt = 2-allylamino-5-methyl-1,3,4-thiadiazole), where the copper atoms are involved in the $[Cu_2(amdt)_2]^{2+}$ units by the formation of σ-donor bonds with the nitrogen atoms of the thiadiazole and π-bonds with the allyl group. The chelate-bridging role of the ligand moiety results in the extreme stability of the $[Cu_2(amdt)_2]^{2+}$dimers, which remain almost unchanged, regardless of the presence of SiF_6^{2-} anions or H_2O molecules in the metal coordination sphere. Furthermore, even crystallization in the presence of acetonitrile, which is known to have a strong affinity for Cu^+ ions, retains these dimers and leads to a structure with non-bonded CH_3CN molecules embedded into the lattice.

Ab-initio quantum-chemical calculations using the DFT/B3LYP/cc-pVDZ approach were used to obtain the equilibrium geometries of two types of $[Cu_2(amdt)_2]^{2+}$ cations, which were marked as the **α**-form and **β**-form for convenience. The difference between these two forms is in the positioning of the allyl groups (see the section Results and Discussion for more details). Optimized geometries were applied as the benchmarks for the Raman spectra calculations. The band assignments of the recorded Raman spectra were made on the basis of the calculated spectra.

4. Experimental Section

4.1 Synthesis of amdt.

The 2-allylamino-5-methyl-1,3,4-thiadiazole was prepared in two steps. First, 4-allylthiosemicarbazide was obtained. A solution of allylisothiocyanate (20.0 mL, 0.206 mol) in 20 mL of ethanol was slowly added through a backflow condenser to intensively cooled by running water solution of hydrazine hydrate (10.0 mL, 0.206 mol) in 10 mL of ethanol. The obtained dense, white suspension was stirred for over 10 min., filtered with suction, washed by ethanol and dried in the air. Recrystallization from acetonitrile yielded white needles of product. Yield: 17.3 g (64%), m.p. 76 °C. In the next stage, 2-allylamino-5-methyl-1,3,4-thiadiazole (***L***) was obtained using the classic Pulvermaher procedure by the reaction of 4-allylthiosemicarbazide with acetyl chloride.[29] An excess of acetyl chloride (8.25 g, 0.105 mol) was added to the powdered 4-allylthiosemicarbazide (3.93 g, 0.03 mol) cooling by cold water to keep the room temperature of the mixture. Then the reaction vessel was equipped with a calcium chloride tube and the mixture was stirred for 20 hours. After this, ice-cold water (20 mL) was poured into the cooled mixture, neutralized with a potassium hydroxide solution (20%) (to pH ≈ 7.5) to precipitate the 2-allylamino-5-methyl-1,3,4-thiadiazole. The crude product was filtered, washed with small

quantities of cold water and recrystallized from the water to yield of 62% (2.89 g). NMR 1H (400 MHz, $CDCl_3$), δ, p.p.m. 6.36 (s, 1H, NH), 5.97–5.87 (m, 1H, =CH), 5.32 (d, *J* = 17.2, 1H, -CH_2-), 5.22 (d, *J* = 10.4, 1H, -CH_2-), 3.94 (d, *J* = 5.6, 2H, CH_2=), 2.57 (s, 3H, CH_3).

4.2 Electrochemical syntheses

The syntheses were performed in small (~10-mm i.d., 5-ml volume) test tubes. A copper wire was wrapped into a spiral of 1-cm diameter, and a straight copper wire was placed inside the spiral. These copper electrodes were inserted into cork and immersed in solutions containing copper(II) hexafluorosilicate and the ligand. Syntheses were performed using an alternating current of 50 Hz applied to both wire electrodes.

The main advantage of such a synthesis route is the one-step growth of high-quality single crystals suitable for X-ray structure experiments. Also, this technique allows the use as starting materials easily accessible and stable Cu^{2+} salts instead of the sensitive-to-oxidation (or even unknown) Cu^{+} derivatives. The electrochemical process does not require additional reducing agents, making the reaction products free from undesirable contaminants.

The main disadvantage of this method is the relatively low yield caused by an abrupt decrease of the electrical conductivity of the electrode(s) due to the appearance of crystalline products at the electrode surface.

4.2.1 Synthesis of $[Cu_2(amdt)_2]SiF_6 \cdot C_6H_6$

A solution of 2-(allyl)-amino-5-methyl-1,3,4-thiadiazole (1.3 mmol, 0.20 g) in a mixture of 3.1 mL of acetonitrile and 0.8 mL of benzene was carefully layered over a 0.8-mL water-saturated solution of $CuSiF_6 \cdot 4H_2O$ (into 5 mL test-tube). The upper layer was transparently yellowish, the lower one was cyan colored. Darkening of the lower part of the acetonitrile-benzene layer, possibly because of diffusion from the water layer, was observed, but it disappeared after the application of the tension. Then copper-wire electrodes in the cork were inserted and colorless crystals of the compound appeared directly on the electrodes under the alternating-current tension [30] (frequency 50 Hz) of 0.60 V after 3 days.

4.2.2 Synthesis of $[Cu_2(amdt)_2(H_2O)_2]SiF_6 \cdot CH_3CONH_2 \cdot 2H_2O$

After a long period (over 2 years) in a closed test tube from a previous synthesis, large well-shaped prismatic crystals of $[Cu_2(amdt)_2(H_2O)_2]SiF_6 \cdot CH_3CONH_2 \cdot 2H_2O$ were found. Evidently, the slow hydrolysis of acetonitrile, used as one of the solvents in the synthesis of $[Cu_2(amdt)_2]SiF_6 \cdot C_6H_6$, is responsible for the acetamide appearance in the compound $[Cu_2(amdt)_2(H_2O)_2]SiF_6 \cdot CH_3CONH_2 \cdot 2H_2O$. Moreover, one more assumption is that a slow water penetration into the acetonitrile-benzene layer and the very slow formation of acetamide results in

a very slow crystallization of $[Cu_2(amdt)_2(H_2O)_2]SiF_6 \cdot CH_3CONH_2 \cdot 2H_2O$ and, consequently, the appearance of good-quality, large (about 2–3 mm in length) crystals.

4.2.3 Synthesis of $[Cu_2(amdt)_2(H_2O)_2]SiF_6 \cdot CH_3CN \cdot 2H_2O$

To 3.2 mL of acetonitrile solution of 2-(allyl)-amino-5-methyl-1,3,4-thiadiazole (1.3 mmol, 0.20 g) 0.8 mL of water-saturated solution of $CuSiF_6 \cdot 4H_2O$ and 0.7 mL of benzene were added. The mixture was carefully stirred. The resulting mixture, consisting of an upper dark layer (based on acetonitrile) and a lower light-green one (based on water), was subjected to alternating-current reduction (frequency 50 Hz, tension 0.50 V) (the acetonitrile layer became fully discolored), and after 3 days good-quality, colorless crystals of $[Cu_2(amdt)_2(H_2O)_2]SiF_6 \cdot CH_3CN \cdot 2H_2O$ appeared on the copper-wire electrodes.

4.3 Crystallography

Single-crystal data for the compound $[Cu_2(amdt)_2]SiF_6 \cdot C_6H_6$ were collected on a Rigaku AFC7 diffractometer equipped with a Mercury CCD area detector, using graphite monochromatized Mo*K*α radiation. The data were treated using the Rigaku CrystalClear software suite program package.[31] The structure was solved by direct methods using the SIR-92 [32] program (teXan crystallographic software package of Molecular Structure Corporation [33]) and refined with SHELXL-97 [34] software, implemented in the program package WinGX.[35] The data for the compounds $[Cu_2(amdt)_2(H_2O)_2]SiF_6 \cdot CH_3CONH_2 \cdot 2H_2O$ and $[Cu_2(amdt)_2(H_2O)_2]SiF_6 \cdot CH_3CN \cdot 2H_2O$ were collected on a Gemini A diffractometer equipped with an Atlas CCD detector, using graphite monochromatized Mo*K*α radiation. The data were treated using the Crysalis software suite program package.[36] The structures were solved using the charge-flipping method and the Superflip [37] program (Olex crystallographic software [38]) and refined with SHELXL-2013 [39] software, implemented in the program package WinGX. [35] The figures were prepared using DIAMOND 3.1 software.[40]

There were some difficulties regarding the structure solution of the compound $[Cu_2(amdt)_2(H_2O)_2]SiF_6 \cdot CH_3CN \cdot 2H_2O$. At first, relatively strong peaks of residual electron density forming an unusual 10-membered cycle with some very short distances were observed on the difference Fourier map. Careful analysis of the interatomic distances and the thermal parameters of the corresponding atoms within such a fragment prompted us to treat these peaks of electron density as a disordered acetonitrile molecule with a common carbon atom of the methyl group for both disordered parts, and two differently oriented cyano-groups with an occupancy of 0.5. Such a model resolves the problem of the too short distances between the symmetrically generated N4…N4’ atoms and explains, in general, the appearance of what appears to be a 10-membered ring. More details are discussed, together with a structure description. CCDC 1054159

for $[Cu_2(amdt)_2]SiF_6 \cdot C_6H_6$, 1054160 for $[Cu_2(amdt)_2(H_2O)_2]SiF_6 \cdot CH_3CONH_2 \cdot 2H_2O$ and 1054161 for $[Cu_2(amdt)_2(H_2O)_2]SiF_6 \cdot CH_3CN \cdot 2H_2O$ contain the supplementary crystallographic data for this paper. These data can be obtained free of charge from The Cambridge Crystallographic Data

4.4 Raman spectroscopy

The Raman spectra were measured on crystals of the coordination compounds and ligand powder with a Horiba Jobin–Yvon LabRAM HR spectrometer using the 632.81-nm excitation line of a He–Ne laser with a power of 17 mW. To avoid decomposition of the sample, a density filter was applied to reduce the power of the laser to 1.7 mW. An Olympus ×50 long-distance lens was used. The spectra were obtained by accumulating 50 scans with an integration time of 5 seconds directly in the air at room temperature. Prior to recording, the spectrometer was calibrated using a Si polycrystalline plate as a standard with a characteristic band at 520.6 cm^{-1}.

4.5 Computational details

For the interpretation of the measured vibrational spectra, *quantum-mechanical* methods were applied. All the calculations were performed using the DFT with the B3LYP functional [41, 42] and cc-PVDZ basis set using the GAMESS(US) program package [43]. All the calculations were carried out using the C1 symmetry group. Effective core potentials (ECPs) were additionally applied for the copper atoms. In order to reduce the complexity of the computation and avoid free shifts of the weakly bonded ligands, which will no doubt contribute to the equilibrium geometry and spectrum, only the $[Cu_2(amdt)_2]^{2+}$ cation was modeled. Initial geometries of the dimeric cations, obtained by an X-ray crystal structure determination of the compounds $[Cu_2(amdt)_2]SiF_6 \cdot C_6H_6$ and $[Cu_2(amdt)_2(H_2O)_2]SiF_6 \cdot CH_3CONH_2 \cdot 2H_2O$, were optimized and the resulting equilibrium geometries were used for the Forces Constants matrix calculation. Then, the polarizability tensors were calculated and the resulting Raman activities (S_i) were converted to Raman intensities (I_i) using the following relationship from the intensity theory of Raman scattering [44, 45] (see equation 1) and normalized to the most intensive band for each spectrum.

$$I_i = \frac{f(v_0 - v_i)^4 S_i}{v_i \left[1 - exp^{\left(-\frac{hcv_i}{kT}\right)}\right]} \qquad (1)$$

v_0 – exciting frequency (cm^{-1})

v_i –vibrational wave number of the i-th normal mode (cm^{-1}).

Acknowledgements.

The authors gratefully acknowledge Slovenian Research Agency (ARRS) for financial support.

Appendix A. Supplementary data.

The following materials are available: CIF files for all the compounds, XYZ files with equilibrium and initial geometries of the **α**- and **β**-forms of $[Cu_2(amdt)_2]^{2+}$, Raman spectrum of $[Cu_2(amdt)_2(H_2O)_2]SiF_6 \cdot CH_3CN \cdot 2H_2O$ demonstrating the band from acetonitrile (Fig. S1)

References

[1] P. Wang, J.-P. Ma, X.-Y. Li, R.-Q. Huang, Y.-B. Dong. Acta Crystallographica Section C, 65 (2009) m78-m81.
[2] Q. Zhang, J.-B. Zhang, L.-H. Cao, Y.-P. Li, D.-Z. Wang. Journal of the Chinese Chemical Society, 57 (2010) 992-997.
[3] Y. Deng, J. Liu, Q. Zhang, F. Li, Y. Yang, P. Li, J. Ma. Inorganic Chemistry Communications, 11 (2008) 433-437.
[4] E.A. Goreshnik, B. Ardan, Y. Slyvka, N. Pokhodylo, M.G. Mys'kiv, in: M.u. Cetina (Ed.) The Twenty-second Croatian-Slovenian Crystallographic Meeting - CSCM22, Book of abstracts and program. Zagreb: Croatian Academy of Sciences and Arts, Croatian Crystallographic Association, Croatian Association of Crystallographers, 2013, Biograd, Croatia, June 12-16, 2013., 2013, pp. 41.
[5] V.V. Olijnyk, E.A. Goreshnik, V.K. Pecharsky, L.I. Budarin, M.G. Mys'kiv. Journal of Structural Chemistry, 34 (1993) 615-621.
[6] E.A. Goreshnik, V.V. Olijnyk, V.K. Pecharsky, M.G. Mys'kiv. Russian Journal of Inorganic Chemistry, 39 (1994) 71-76.
[7] A.A. Shkurenko, V.N. Davydov, M.G. Mys'kiv. Russian Journal of Coordination Chemistry, 32 (2006) 270-275.
[8] E.A. Goreshnik, M.G. Mys'kiv. Journal of Chemical Crystallography, 4 (2010) 381-383.
[9] E.A. Goreshnik, Y.I. Slyvka, M.G. Mys'kiv. Inorganica Chimica Acta, 377 (2011) 177-180.
[10] B. Ardan, Y. Slyvka, E. Goreshnik, M. Mys'kiv. Acta Chimica Slovenica, 60 (2013) 484–490.
[11] Y. Slyvka, N. Pokhodylo, R. Savka, E. Goreshnik, Z. Mazej. Chemistry of Metals and Alloys, 2 (2009) 130-137.
[12] Y. Slyvka, N. Pokhodylo, R. Savka, Z. Mazej, E. Goreshnik, M. Mys'kiv. Chemistry of Metals and Alloys, 3 (2010) 201-207.
[13] V.V. Olijnyk, E.A. Goreshnik, D. Schollmeyer, M.G. Mys'kiv. Russian Journal of Coordination Chemistry, 23 (1997) 548.
[14] F.H. Jardine, L. Rule, A.G. Vohra. Journal of the Chemical Society A: Inorganic, Physical, Theoretical, (1970) 238-240.
[15] D.J. Gulliver, W. Levason, M. Webster. Inorganica Chimica Acta, 52 (1981) 153-159.

[16] A. Banu, R.S. Lamani, I.A.M. Khazi, N.S. Begum. Journal of Saudi Chemical Society, 18 (2014) 371-378.
[17] S.-i. Noro, T. Ohba, K. Fukuhara, Y. Takahashi, T. Akutagawa, T. Nakamura. Dalton Transactions, 40 (2011) 2268-2274.
[18] H.V.R. Dias, H.-L. Lu, H.-J. Kim, S.A. Polach, T.K.H.H. Goh, R.G. Browning, C.J. Lovely. Organometallics, 21 (2002) 1466-1473.
[19] A.K. Barnard, Theoretical Bases of Inorganic Chemistry, McGraw-Hill, New-York 1965.
[20] J.L. Duncan. Mol. Phys., 28 (1974) 1177-1191.
[21] R.J. van der Wal, A. Vos. Acta Crystallographica Section B, 38 (1982) 2318-2320.
[22] L. Strzemecka, D. Maciejewska, Z. Urbańczyk-Lipkowska. Journal of Molecular Structure, 648 (2003) 107-113.
[23] X. Rui-Bo, X. Xing-You, W. Ming-Yan, Y. Xu-Jie, W. Xin, L. La-De, M. Wei-Xing, Chinese Journal of Structural Chemistry, 28 (2009) 703-707.
[24] A.-G. Yu, M. Zhang, G.-D. Yang, L. Ye, Y.-G. Ma. Acta Crystallographica Section E, 65 (2009) m875.
[25] Y.I. Slyvka, E.A. Goreshnik, B.R. Ardan, G. Veryasov, D. Morozov, M.G. Mys'kiv. Journal of Molecular Structure, 1086 (2015) 125-130.
[26] T. Shimanouchi, 1972, Tables of Molecular Vibrational Frequencies Consolidated, National Bureau of Standard, 1972.
[27] J.M. Dudik, C.R. Johnson, S.A. Asher.The Journal of Physical Chemistry, 89 (1985) 3805-3814.
[28] A. Ouasri, A. Rhandour, M.-C. Dhamelincourt, P. Dhamelincourt, A. Mazzah. Spectrochimica Acta Part A: Molecular and Biomolecular Spectroscopy, 59 (2003) 357-362.
[29] G. Pulvermacher. Berichte der deutschen chemischen Gesellschaft, 27 (1894) 613-630.
[30] B.M. Mykhalichko, M.G. Mys'kiv, Ukraine Patent UA 25450A, Bull. № 6, (1998).
[31] Rigaku Corporation, CrystalClear, The Woodlands, Texas, USA, (1999).
[32] A. Altomare, G. Cascarano, C. Giacovazzo, A. Guagliardi. Journal of Applied Crystallography, 26 (1993) 343-350.
[33] Crystal Structure Analysis Package, Molecular Structure Corporation, teXan for Windows, version 1.06, (1997-9).
[34] G. Sheldrick. Acta Crystallographica Section A, 64 (2008) 112-122.
[35] L. Farrugia. Journal of Applied Crystallography, 32 (1999) 837-838.
[36] Agilent Technologies, CrysAlisPro, Version 1.171.37.31 (release 14−01−2014 CrysAlis171 .NET)
[37] L. Palatinus, G. Chapuis. Journal of Applied Crystallography, 40 (2007) 786-790.
[38] O.V. Dolomanov, L.J. Bourhis, R.J. Gildea, J.A.K. Howard, H. Puschmann. Journal of Applied Crystallography, 42 (2009) 339-341.
[39] G. Sheldrick. Acta Crystallographica Section C, 71 (2015) 3-8.

[40] DIAMOND v3.1., Crystal Impact GbR, Bonn, Germany, (2004-2005).
[41] A.D. Becke. The Journal of Chemical Physics, 98 (1993) 5648-5652.
[42] C. Lee, W. Yang, R. Parr. Physical Review B, 37 (1988) 785-789.
[43] M.W. Schmidt, K.K. Baldridge, J.A. Boatz, S.T. Elbert, M.S. Gordon, J.H. Jensen, S. Koseki, N. Matsunaga, K.A. Nguyen, S. Su, T.L. Windus, M. Dupuis, J.A. Montgomery. Journal of Computational Chemistry, 14 (1993) 1347-1363.
[44] P.L. Polavarapu. The Journal of Physical Chemistry, 94 (1990) 8106-8112.
[45] G. Keresztury, S. Holly, G. Besenyei, J. Varga, A. Wang, J.R. Durig. Spectrochimica Acta Part A: Molecular Spectroscopy, 49 (1993) 2007-2026.

Highlights:

- Three novel copper(I) hexafluorosilicate π-complexes with amdt ligand are prepared
- Single crystal X-ray diffraction revealed two geometries of $[Cu_2(amdt)_2]^{2+}$
- Chelate-bridging role of the ligand leads to extreme stability of $[Cu_2(amdt)_2]^{2+}$
- Raman spectra were analyzed on the basis of quantum-chemical calculations